

34. PETROGRAPHY OF CALCITE VEINS IN SERPENTINIZED PERIDOTITE BASEMENT ROCKS FROM THE IBERIA ABYSSAL PLAIN, SITES 897 AND 899: KINEMATIC AND ENVIRONMENTAL IMPLICATIONS¹

Julia K. Morgan² and Kitty L. Milliken³

ABSTRACT

Calcite veins recovered from serpentinized peridotite and serpentinite breccia basement rocks at Sites 897 and 899 reveal a complex history of fracturing and carbonate precipitation in an extensional environment related to the rifting of the North Atlantic. Crosscutting and textural relationships among the veins suggest a progression of carbonate vein-filling events in open fractures, involving the growth of acicular aragonite, subsequently altered mostly to calcite, followed by the precipitation of botryoidal, fibrous calcite, and finally by highly zoned, sparry calcite. The morphological progression may arise from changes in carbonate precipitation rate, possibly associated with temporal variations in vein width. At Site 897 (and rarely at Site 899), this sequence is crosscut by micrite-filled veins resembling neptunian fractures, composed of remobilized calcite, oxides, and serpentinite fragments, which may be derived from the in situ brecciation of the wall rock. The vein complexes, and complicated cracking, resealing, and crosscutting textures, are probably the result of a series of discrete, brittle dilational events associated with the late stages of uplift and exposure of serpentinized peridotite basement at the seafloor. The final fracture event, producing the micrite-filled veins, may have resulted from gravitational collapse of the uplifted blocks, perhaps culminating locally in complete brecciation and subsequent mass flow.

INTRODUCTION

Alteration of serpentinized peridotites in a rifted margin setting produces authigenic minerals that, potentially, may record fluid/rock interactions over greatly varied temperatures, fluid compositions, and fluid flow conditions. At one end of this spectrum, conditions affiliated with the initial serpentinization of the rising peridotite produce mineral assemblages characteristic of several hundred °C temperatures and many kilometers of burial (e.g., alteration described for Leg 103 peridotites by Agrinier et al., 1988; Kimball and Evans, 1988). Contrasting possibilities for alteration of serpentinitic materials include weathering on the seafloor (e.g., Gillis and Robinson, 1988) or even meteoric weathering early in rifting, before the ultimate incursion of seawater into the rift valley, a scenario proposed by Folk and McBride (1976) for ophicalcites in Italy. Strong overprinting of primary chemical indicators characterizes ophicalcites brought to the surface through compressional deformation (e.g., Weissert and Bernoulli, 1984; Früh-Green et al., 1990). Carbonate-enriched ultramafic rocks at mid-ocean ridges lack this sort of tectonic overprint and have yielded many insights into the origin of ophicarbonates (e.g., Bonatti et al., 1974; 1980). Calcitized serpentinitic rocks at Sites 897 and 899 provide further opportunity to investigate the nature of interactions between mantle rocks and shallow hydrous environments during rifting without the compositional and textural overprint of subsequent compressional tectonics.

Shipboard observations of the numerous veins preserved in basement rocks at Sites 897 and 899 revealed complex lithologic and textural variations and crosscutting relationships among the veins (Saw-

yer, Whitmarsh, Klaus, et al, 1994). A detailed petrographic examination of the carbonate vein occurrences is undertaken in this study, using standard optical microscopy and optical microscope-based cathodoluminescence to delineate the kinematic history and environmental conditions associated with the late brittle deformation of the basement rocks at these two sites. Petrographic observations reveal a complex history of fracture, precipitation, and vein healing, which correlates roughly with a sequence of carbonate phases and textures deposited in open veins. We interpret this sequence to reflect the progressive exposure and dilation of the basement blocks during rifting, perhaps accompanied by associated changes in carbonate precipitation conditions (e.g., precipitation rate) producing the morphologic progression. In a companion paper, Milliken and Morgan (this volume) use isotopic and trace-elemental analyses to argue that the present vein-filling calcites precipitated near the seafloor from fluids derived from ambient Early-to-middle Cretaceous seawater.

GEOLOGIC SETTING

Sites 897 and 899 were drilled on basement highs at the ocean-continent transition in the Iberia Abyssal Plain. The recovery of serpentinized peridotite at both sites supports the interpretation that basement in this setting represents unroofed, altered mantle peridotite exposed in a transition zone during Early Cretaceous rifting of the north Atlantic (e.g., Whitmarsh et al., 1993; Shipboard Scientific Party, 1994a). The origin of the regional basement highs within the transition zone at the Iberia Abyssal Plain is not well understood (e.g., Shipboard Scientific Party, 1994b), but analogous serpentinite peridotite ridge exposures along the Galicia margin have been attributed to diapiric rise and subsequent tectonic denudation of serpentinized mantle rocks during asymmetric rifting (Boillot et al., 1988). Basement cores at Site 897 revealed apparently in situ serpentinized peridotite, which displays some relict crystalline textures, mantled by a 30- to 40-m-thick chaotic mix of various sedimentary, serpentinized, and other crystalline lithologies interpreted to be mass flow deposits

¹Whitmarsh, R.B., Sawyer, D.S., Klaus, A., and Masson, D.G. (Eds.), 1996. *Proc. ODP, Sci. Results*, 149: College Station, TX (Ocean Drilling Program).

²Department of Geological Sciences, University of Washington, Seattle, WA 98195, U.S.A. morgan@geology.washington.edu.

³Department of Geological Sciences, University of Texas, Austin, TX 78712, U.S.A.

(Shipboard Scientific Party, 1994b). At Site 899, in situ basement rock was never unequivocally recovered; acoustic basement consisted of up to 100-m-thick, coherent, serpentinitized peridotite breccia units, intercalated with similar lithologic mixtures as observed at Site 897 (Shipboard Scientific Party, 1994c). Microfossil ages determined from the intercalated sediments indicated a normal stratigraphic succession ranging in age from Barremian-Aptian to Campanian-Maastrichtian (Shipboard Scientific Party, 1994b), temporally associated with the early stages of continental break-up in the Iberia Abyssal Plain (Whitmarsh et al., 1990). The serpentinite breccias are interpreted to be massive landslide or debris flow deposits (Gibson, Milliken, and Morgan, this volume). They are by nature very homogeneous, essentially monomineralic, unsorted, and display a dominantly brittle texture (Shipboard Scientific Party, 1994c). The high degree of lithification of the breccias is attributed to postdepositional cementation, as yet unidentified (authigenic clay or serpentine). The character of the breccias is in sharp contrast to that of the underlying sediments, which, although varied, are typically uncompacted, uncemented, and contain few if any veins.

Acoustic basement at both sites displays downhole chemical trends, attributed in part to near-seafloor weathering and alteration. The more altered rocks near the tops of the basement units show greater oxidation, increased porosity, and higher concentrations of calcite from a combination of mineral replacement and pervasive fracture and vein filling (Gibson, Milliken, and Morgan, this volume); the most highly weathered basement samples tend to disaggregate easily, and contain significant quantities of authigenic clay (Milliken et al., this volume).

MACROSCOPIC DESCRIPTION OF VEINS

Calcite veins at both Site 897 and 899 are found dominantly in the upper sections of the basement and are observed to overprint serpentine veins at Site 897 (Shipboard Scientific Party, 1994c). At Site 899, serpentine veins occur exclusively within clasts, denoting a vein-filling phase that predated fragmentation and transport of the breccia units to their final resting place. Calcite veins, although found throughout the crystalline lithologies, are concentrated in Cores 899-18R-21R, coincidentally correlating with the greatest abundance of large clasts in the core (Shipboard Scientific Party, 1994c).

There are several recurring types of calcite veins, distinguished by their macroscopic appearance. The large veins are most distinctive and take three main forms. *Zoned veins* are most common at Site 899, but also occur at Site 897. They display an approximately planar geometry, and are marked by subparallel bands of inclusions and color variations grading into clear, coarsely crystalline, sparry calcite near the center of the vein. These features may reach 5 cm across (Fig. 1A). *Sheeted veins* are so called because they constitute several subparallel veins with various textures, separated by thin bands of wall rock or noncarbonate phases (Fig. 1B). These features tend to develop at the margins of large clasts, possibly because of contrasts in strength between clast and breccia. They are only observed at Site 899. *Complex veins* include most of the larger vein types recovered from Site 897, are poorly correlated among samples, and encompass multiple vein textures in a chaotic package. One of the most distinctive textures observed in abundance in these vein types, particularly at Site 897, is a relict aragonite texture replaced by sparry calcite (Fig. 2). More pervasive at both sites are *fine, clear veins*. They are most common in the upper reaches of basement, where they permeate the disaggregated breccia. They often occur in subplanar, anastomosing sets, or as circumgranular features. At Site 897, similar fine calcite veins define the familiar serpentinite mesh texture near the seafloor, but revert to serpentine filling with depth (Shipboard Scientific Party, 1994b). *Micrite-filled veins*, common at Site 897, but rare at Site 899, display a clastic texture, dominated by microcrystalline calcite but also containing material apparently derived from local fragmentation

of the serpentinite and its alteration phases. The detritus-filled fractures postdate most other vein generations with which they occur (Fig. 3). These features bear some resemblance to neptunian fractures, recognized elsewhere in extensional or collapse settings (e.g., Smart et al., 1987), an analogy that may bear on their genesis in this setting.

The high degree of fragmentation and relative rotation of unoriented cores, particularly at Site 897, confound efforts to establish an orientation distribution of the vein occurrences at both sites, useful for kinematic inferences. Casual observations, however, indicate that the vein orientations are quite variable, even within a single core, and appear to be largely controlled by preexisting rock fabrics (e.g., foliation, serpentine veins, margins of clasts). The implication is that fracturing in these heterogeneous rocks was governed largely by local stress concentrations in response to a general dilational tendency.

SAMPLING AND METHOD OF STUDY

Petrographic analysis was conducted on a suite of 34 samples, chosen as representatives of the variety of calcite veins observed in basement cores from Sites 897 and 899. The list of samples studied is given in Table 1, along with a brief petrographic description based on the discussion in the text. Before sectioning, thin-section billets were impregnated with blue-dyed epoxy to make existing porosity more visible. Standard petrographic examination was performed using several optical microscopes. Cathodoluminescence imaging was performed using a Premier American Technologies Luminoscope (model ELM-3R) mounted on a Leitz brand Ortholux microscope. Operating voltage and current were set at 10 kV and 0.4 mA, respectively.

A subset of the petrographic samples described herein was subsequently used for isotopic and trace-elemental analysis, using photographic maps of features noted during petrographic and cathodoluminescence examination. The analyses that were performed are detailed in Table 1, and the results and interpretations of this chemical study are presented in an accompanying paper by Milliken and Morgan (this volume).

MICROSCOPIC DESCRIPTION OF VEINS

Petrographic examination of the vein samples revealed a varied array of calcite habits and multiple crosscutting, truncation, and replacement textures, demonstrating a complex history of vein fracture, precipitation, and sealing. Several textures recur in many veins of various types and can be correlated to reveal a progression of features useful for extracting basement history. The common occurrences are presented in approximate order of their appearance in the rocks.

Calcite Textures

Aragonite and Calcite Pseudomorphs after Aragonite

Equant, unoriented, clear sparry calcite, occurring in elongate to prismatic sections within a more varied matrix, points to the presence of relict aragonite in several complex veins from Site 897 (e.g., Figs. 2, 4). In places, these features occur as radiating stellate clusters centered on the vein wall, with preserved crystal outlines consistent with coarse, bladed aragonite (B. Kirkland-George, pers. comm., 1994). Embayed faces serve as nucleation sites for later, infilling botryoidal calcite, which also fills fractures in the now-replaced bladed crystals, demonstrating that aragonite represents the earlier phase. The presence of primary aragonite in some samples (e.g., Sample 149-897D-16R-4, 0-5 cm) supports the interpretation that these textures preserve an early phase of aragonite precipitation in open fractures. This relict aragonite texture was generally absent in veins at Site 899 with one exception: Sample 149-899B-17R-2, 91-94 cm, revealed elon-

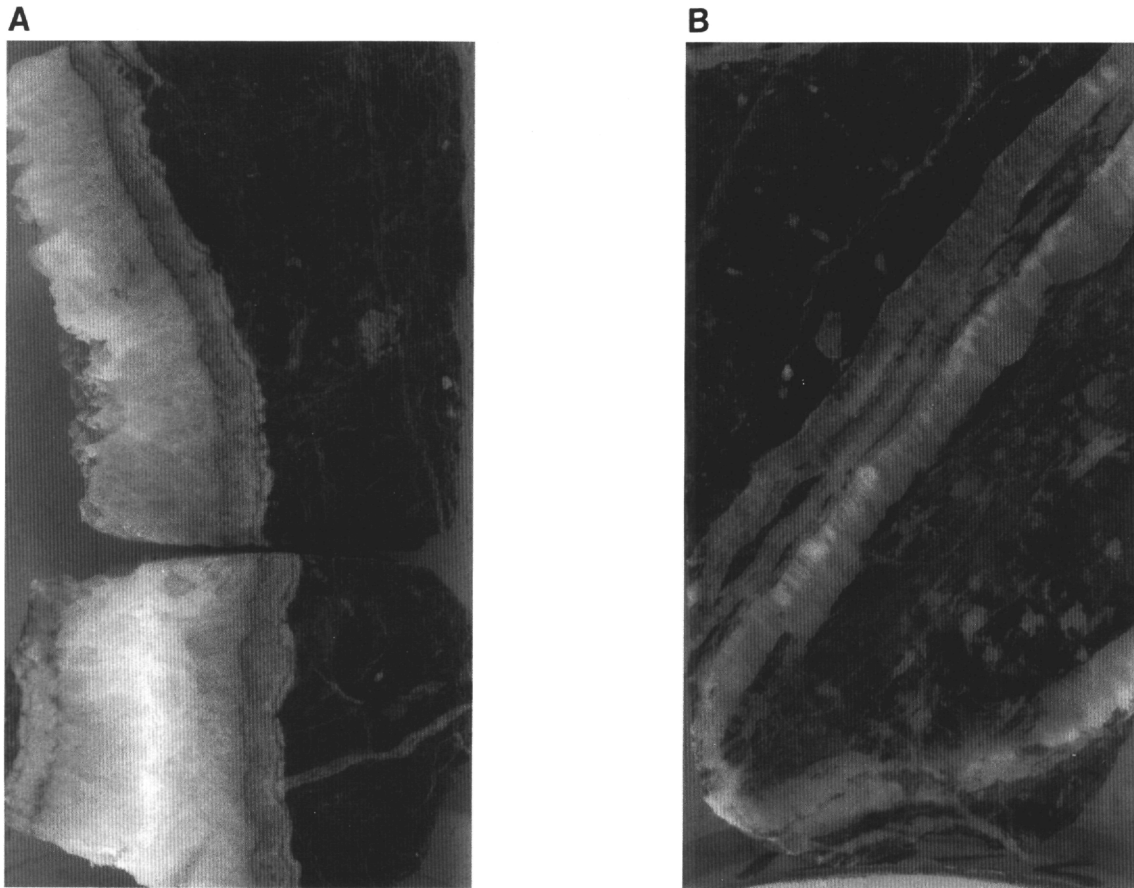


Figure 1. Common carbonate-filled vein types. **A.** Zoned vein, as displayed in Sample 149-899B-20R-1, 25-36 cm, exhibits color and inclusion banding subparallel to vein walls, grading to relatively coarse sparry calcite near the center of the vein. This vein type is observed at both Sites 897 and 899. **B.** Sheeted vein complexes, displayed in Sample 899B-18R-2, 0-11 cm, consist of several subparallel veins with varied textures (e.g., fibrous, botryoidal, blocky), separated by fragments of wall rock or deposits of noncarbonate phases (e.g., oxides, chlorite). These complexes frequently form at the boundaries of large clasts within the breccia, and are more common at Site 899.

gate, radiating blades reminiscent of aragonite in a complex vein which was subsequently crosscut by several zoned and fibrous veins.

Botryoidal Calcite

Radiating, fibrous clusters of calcite, nucleated at the vein wall or along an earlier carbonate phase, define a common botryoidal habit observed in many vein types at both Sites 897 and 899. Much of the botryoidal calcite is highly vacuolized. The gas-filled vacuoles are on the order of 1 μm across and may occur in relatively uniform concentrations or form concentric rings about the core. The most highly vacuolized samples are prominently white in reflected light. Less vacuolized examples occur, and crosscutting relationships suggest that the less vacuolized botryoidal calcite may be older (e.g., Sample 149-899B-25R-3, 21-24 cm). Typically, this phase is highly luminescent, with the intensity of luminescence correlating positively with the density of inclusions. Calcite fibers appear to have grown in fan-like arrays into open fractures, in many cases nearly sealing the vein. Postprecipitation fractures confirm the early paragenesis of the vacuolized calcite. Later fractures often localize between individual clusters, and are subsequently filled by clear sparry calcite (Fig. 5). Much of the subsequent fracturing is also localized along the contact of the botryoidal calcite with the fracture wall, truncating and displacing the radial clusters.

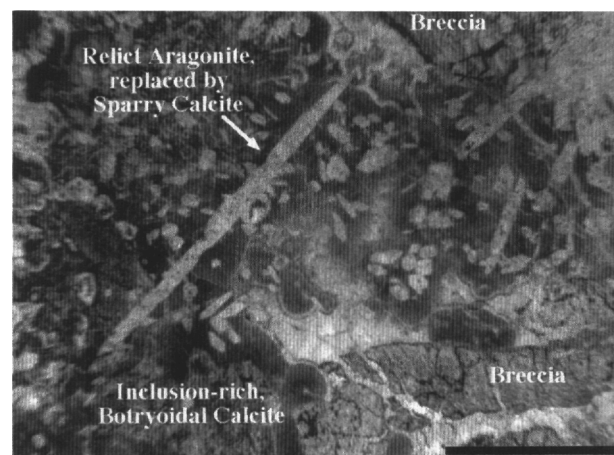


Figure 2. Chaotic vein in Sample 149-897D-16R-3, 17-19 cm. This image shows relict aragonite texture replaced by clear, sparry calcite, which appears to slash across all other calcite phases. Aragonite is interpreted to be the earliest phase in this sample, with vacuolized, botryoidal calcite grading to zoned sparry calcite cementing the crystals. Other calcite morphologies are also recognized in this sample, but relationships among the many phases are difficult to ascertain. Scale bar is 5 mm long.

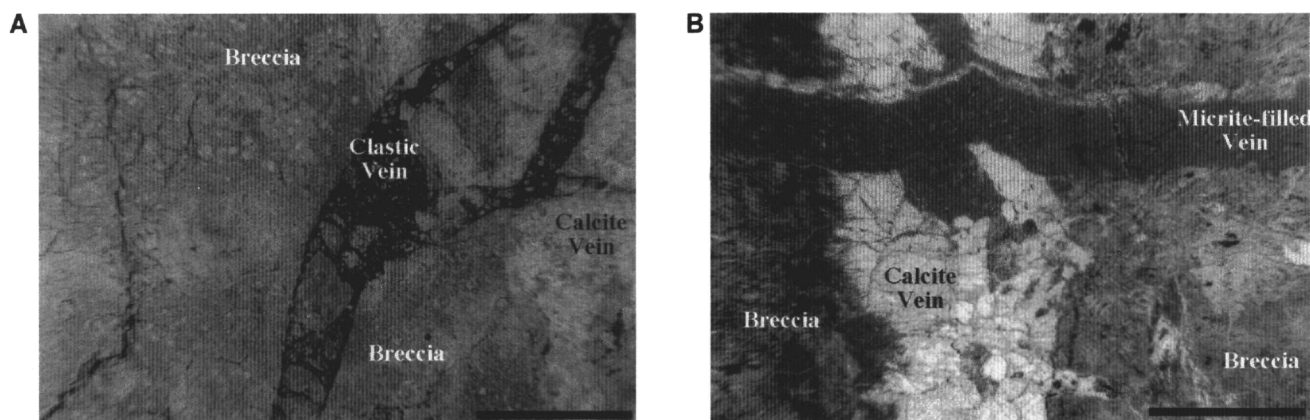


Figure 3. Two micrite-filled veins displaying clastic texture from Site 897. **A.** Plane-polarized light image of a highly oxidized vein in Sample 149-897D-13R-5, 57-61 cm, containing fragments of brecciated serpentinite. The clastic vein is observed to cut a calcite vein at the right side of the image. Scale bar is 5 mm long. **B.** Plane-polarized light image of a relatively homogeneous micrite-filled vein in Sample 149-897C-64R-4, 16-19 cm, which cuts across a large vein grading from vacuolized botryoidal calcite at the margins to clear, sparry calcite in the center. Clear, fibrous to sparry calcite is observed to postdate the emplacement of the micrite-filled vein; a thin vein parallels the top edge of the clastic vein and crosscuts a protrusion. Several perpendicular fibrous veins also cut the micrite-filled vein to the right of its intersection with the large vein. Scale bar is 5 mm long.

Zoned Sparry Calcite

The most common calcite texture observed in many veins takes the form of elongate blades, oriented perpendicular to the vein walls and growing into open fractures. The crystal facets of the dogtooth spar are still preserved at the edges of open porosity, and elsewhere result in a jagged suture where crystals growing from opposite sides of the wall meet. Blades typically coarsen inward, as more favorably oriented crystals occlude others. The calcite is highly zoned, grading from alternating bands of inclusions with variable luminescence close to the wall (Fig. 6A-C), to uniform, clear calcite displaying fine rhythmic luminescent zoning of decreasing intensity near the center (Fig. 6D-F). This calcite type dominates veins at both sites, although it is best developed in the zoned veins at Site 899. Precipitation of this sparry calcite is observed to postdate the botryoidal phases, occurring along the truncated boundaries (e.g., Sample 149-899B-18R-2, 135-139 cm), or, in places, apparently syntaxial to the botryoids (e.g., Sample 149-897D-16R-3, 17-19 cm). Fluid-filled inclusions ranging from 10 to 50 μm in size are common in the clear, sparry calcites. No two-phase (fluid-gas) inclusions were observed, which is consistent with the interpreted low temperatures of precipitation.

Fibrous Calcite (Common)

This ubiquitous texture is found throughout the calcite-bearing basement cores at the two sites and occurs both in abundant, narrow veins (Fig. 7), and as a late-stage vein-filling near the margins of the larger sheeted and zoned veins. Fibrous veins are particularly pervasive near the tops of the basement units, where the primary basement mineralogy has undergone significant weathering and alteration, and they commonly show a circumgranular distribution. The texture is marked by fine, clear calcite fibers, although the center of the vein may contain abundant vacuoles, possibly correlated with earlier, highly vacuolized calcite exposed in the larger veins. The fibers are typically oriented perpendicular to the vein wall, show little change in orientation across the vein, and indicate displacive, antitaxial growth from center to wall. Luminescence varies both within and among the veins, demonstrating complicated fracture and growth histories. Timing relationships are very difficult to establish, as veins with this texture appear to have formed throughout much of the evolution of these rocks.

Massive Fibrous Calcite

Few vein samples, notably Samples 149-899B-18R-2, 3-7 cm, and 149-899B-18R-5, 58-62 cm, are marked by a related calcite texture, distinguished by massive (up to 1 cm) generations of relatively homogeneous, clear fibrous calcite. In each case, this texture is observed as a marginal phase, and suggests displacive, antitaxial growth; occurrences are bounded internally by calcites of more blocky or sparry appearance. Luminescence varies little across the domains, so it is difficult to establish their histories. In Sample 149-899B-18R-2, 3-7 cm, this extensive zone of fibrous calcite grades upward into narrow fibrous veins, which displace thin peels of a highly altered serpentinite clast; this hints that the massive fibrous phase is simply a well-developed example of the common veins. However, in this sample it occurs with fibrous silica, a unique occurrence in this suite of veins.

The massive fibrous calcite in Sample 149-899B-18R-5, 58-62 cm, is more enigmatic. The calcite is intergrown with a coarse, fibrous or platy brown phyllosilicate (probably chlorite), with a fabric that suggests that the calcite is replacing an earlier vein-filling phase (Fig. 8). Fiber orientations of the calcite mimic those of the phyllosilicate; kinks in the phyllosilicate are matched by kinks in the calcite. Calcite also occurs as fine beads that grow at the edges of the phyllosilicate laths and may cut across cleavage (Fig. 8). The fibrous calcite is not sharply bounded by other phases, but rather grades toward the center of the vein into clear sparry calcite. Elsewhere, similar intimate relationships between calcite and phyllosilicate are observed, but the fibrous habit is not always evident (e.g., Sample 149-899B-20R-1, 121 cm).

Micrite-filled Veins

Numerous, narrow- to medium-width, clastic-textured veins, ranging in size from 50 μm to 5 mm, crosscut earlier vein-filling phases (including other micrite-filled veins), particularly complex veins noted at Site 897 (e.g., Fig. 3). These typically contain microcrystalline calcite, mixed with fragments of serpentinite, oxides, and pieces of preexisting vein-filling calcite (e.g., Sample 149-899B-35R-1, 32-36 cm). The relative importance of the different constituents can vary from vein to vein, from nearly pure micrite (Sample 149-897C-64R-4, 16-19 cm) to well-oxidized veins with high con-

Table 1. Calcite vein samples chosen from Sites 897 and 899 for petrographic examination and chemical analysis.

Core, section, interval (cm)	Sample depth (mbsf)	Major petrography	Chemical analyses (num.)
149-897C-64R-4, 16–20	661.53	Vacuolized, botryoidal to sparry calcite vein, crosscut by microcrystalline clastic vein.	Fe, Mg, Mn, Sr (29), C, O-isotope (5), Sr-isotope (1) C, O-isotope (1)
65R-1, 19–23	668.19	Anastomosing, subparallel fibrous veins; crosscut clay vein.	
65R-1, 92–94	668.92	Thick zone of crystalline calcite with serpentinite fragments, juxtaposed against highly veined serpentinite.	
149-897D-11R-4, 23–25	698.38	Chaotic intersecting veins, with radiating calcite growths.	C, O-isotope (1)
12R-1, 63–65	704.13	Chaotic, fine-grained calcite with relict aragonite texture, crosscut by microcrystalline clastic vein.	C, O-isotope (1), Sr-isotope (1)
13R-5, 58–62	718.64	Vacuolized, botryoidal calcite truncated by sparry calcite, cut by oxidized clastic vein.	
16R-3, 17–19	743.83	Thick, chaotic vein with sparry calcite after aragonite embedded in botryoidal-sparry calcite.	
16R-3, 132–136	744.98	Vacuolized, botryoidal to sparry vein crosscut by vacuolized calcite vein. Contains primary aragonite.	
16R-4, 0–5	745.15	Clear, blocky calcite with relict & primary aragonite, cut by vacuolized calcite and clear, fibrous vein.	Fe, Mg, Mn, Sr (9), C, O-isotope (1), Sr-isotope (1)
16R-4, 114–116	746.29	Vacuolized, botryoidal to sparry calcite in intersecting veins, with abundant oxides at margins.	Fe, Mg, Mn, Sr (19), Sr-isotope (1)
16R-5, 46–50	747.03	Complicated vein with relict aragonite in botryoidal to sparry calcite, cut by clastic veins and finally clear calcite.	
17R-4, 110–114	756.77	Brucite vein with relict aragonite replaced by sparry calcite; margins are vacuolized calcite.	Fe, Mg, Mn, Sr (6)
17R-6, 62–65	758.40	Intersection of serpentinite-bearing, clastic calcite veins adjacent to brecciated serpentinite mesh.	Sr-isotope (1)
149-899B-16R-1, 69–72	371.81	Vacuolized, botryoidal to sparry calcite followed by fibrous veins.	Fe, Mg, Mn, Sr (58), C, O-isotope (2)
16R-3, 75–78	370.56	(Not examined)	Fe, Mg, Mn, Sr (8)
16R-4, 102–105	374.20	Vacuolized botryoidal to sparry calcite followed by fibrous veins and clear, blocky calcite vein.	Fe, Mg, Mn, Sr (22), C, O-isotope (1)
17R-1, 82–84	380.22	(Not examined)	Fe, Mg, Mn, Sr (11)
17R-2, 91–94	381.74	Chaotic, vacuolized calcite with relict aragonite cut by zoned, vacuolized, botryoidal to sparry calcite.	Fe, Mg, Mn, Sr (46)
17R-2, 91–94	381.74	Chaotic, vacuolized calcite with relict aragonite cut by zoned vacuolized, botryoidal to sparry calcite.	Fe, Mg, Mn, Sr (46)
17R-3, 73–76	(Not examined)	(Not examined)	Fe, Mg, Mn, Sr (13)
18R-1, 74–76	389.84	(Not examined)	Fe, Mg, Mn, Sr (19)
18R-2, 3–7	390.23	Sheeted vein complex with massive, clear, fibrous calcite, botryoidal calcite, and blocky, clear calcite.	Fe, Mg, Mn, Sr (16)
18R-2, 135–139	391.55	Zoned, vacuolized, botryoidal calcite followed by vacuolized to clear, sparry calcite, cut by clear calcite.	Fe, Mg, Mn, Sr (18)
18R-5, 58–62	394.82	Massive clear calcite replacing chlorite, grading into clear sparry calcite with isolated breccia pieces.	Fe, Mg, Mn, Sr (18)
19R-2, 4–8	399.75	Vacuolized, botryoidal calcite crosscut by vacuolized, sparry calcite, followed by clear, fibrous calcite.	
19R-2, 111–114	400.82	Zoned, vacuolized, botryoidal to sparry calcite intersecting multiple generations of fibrous calcite.	Fe, Mg, Mn, Sr (9)
20R-1, 21–24	407.91	Zoned, vacuolized, botryoidal to sparry calcite veins crosscut by clear calcite.	Fe, Mg, Mn, Sr (17), C, O-isotope (3), Sr-isotope (2)
20R-1, 121A	408.91	Sheeted vein complex with vacuolized to clear calcite, blocky, clear calcite with chlorite, and fibrous calcite.	Fe, Mg, Mn, Sr (8)
20R-1, 126A	410.44	Vacuolized, botryoidal calcite, and fibrous to sparry calcite with chlorite.	
20R-2, 16–20	409.34	Botryoidal, zoned, isotropic to microcrystalline chlorite replaced by sparry and vacuolized, botryoidal calcite.	
20R-2, 126–130	410.44	Botryoidal, isotropic zoned chlorite replaced by vacuolized, botryoidal to blocky calcite.	
21R-2, 43–46	418.67	Sheeted vein complex with clear blocky calcite intergrown with chlorite, and coarse to finely fibrous calcite veins.	
22R-1, 59–62	426.89	(Not examined)	Fe, Mg, Mn, Sr (6)
23R-1, 50–52	436.10	Zoned, vacuolized to clear, sparry calcite crosscut by clear fibrous calcite.	
23R-3, 15–18	438.63	Zoned, vacuolized to clear, sparry calcite with crosscutting clear calcite.	
24R-1, 31–34	445.61	Clear, blocky, equigranular calcite with clear, fibrous calcite veins.	
24R-1, 64–67	445.94	(Not examined)	Fe, Mg, Mn, Sr (6)
24R-3, 128–130	449.54	Clear, blocky, equigranular calcite with clear, fibrous calcite veins.	
25R-3, 21–24	457.68	Vacuolized calcite crosscut by zoned, botryoidal to sparry calcite with related fibrous veins.	Fe, Mg, Mn, Sr (16)
28R-1, 69–73	483.59	Clear, fine to coarse, blocky calcite.	
29R-1, 77–82	492.87	(Not examined)	Fe, Mg, Mn, Sr (4)

Notes: Chemical analyses were also performed on several samples not used for the petrographic study; the types of analyses performed are indicated here (number of analyses in parentheses). The results of these analyses are presented in an accompanying paper (Milliken and Morgan, this volume). Petrographic terms are introduced in the text. (Not examined) = Samples that were not available for petrographic study.

centrations of wall rock (Sample 149-897D-13R-5, 57–61 cm). Luminescence of these veins is typically relatively high and uniform for the calcite component.

The origin of these veins remains equivocal. The clastic textures are reminiscent of neptunian veins, which are interpreted to form close to the seafloor in dilational or collapsed karst environments and consequently are open to marine sediment influx (Smart et al., 1987; Winterer et al., 1991). In contrast to those occurrences, however, geotectonic fabrics and microfossils are not evident in our clastic veins. The granular and polymict nature of micrite-filled veins, however, does argue for transport and redeposition of clastic material in open fractures, possibly under dynamic fluid flow conditions (e.g., Hsü, 1983), and the close association of these veins with zones of intense in situ brecciation suggests a likely local source for the vein-filling material. Our sampling is not complete enough to establish the exact relationship between the two clastic modes.

Other Calcite Textures

Other calcite textures observed in the basement cores may also record important events in the fracture and precipitation history, but their relative timing and evolution are much less apparent. Examples include first, clear, medium-course grained, equant calcite with uniform luminescence; second, finely bladed, sparry calcite with uniform luminescence; and third, small, radial aggregates of calcite in complex veins at Site 897. The luminescent properties of these phases tend to be very uniform, possibly because of postprecipitation replacement.

Other Vein Phases

Various noncarbonate phases occur within the calcite veins, perhaps preserving part of the history of vein formation. Several appear

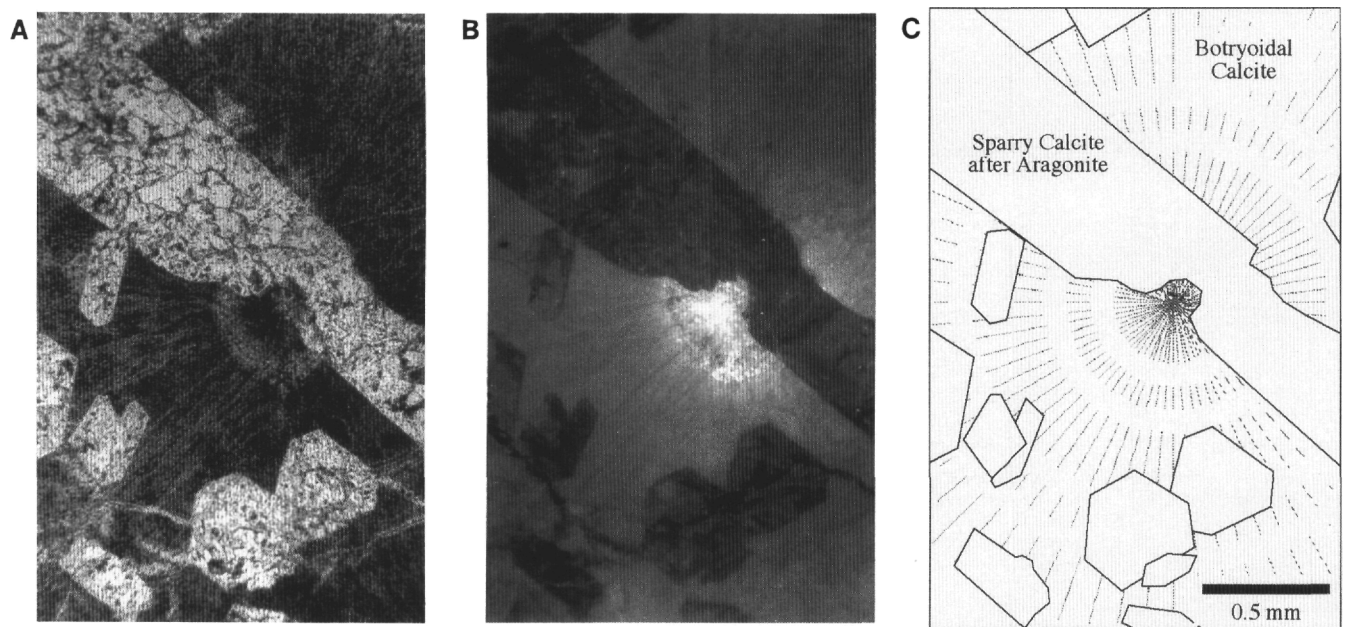


Figure 4. Relict, acicular aragonite crystals replaced by clear, sparry calcite identified in a chaotic vein in Sample 149-897D-17R-6, 62-65 cm. The matrix is composed of later botryoidal calcite, which has nucleated along the embayed face of the aragonite crystal and grown into open space between the crystals. **A.** Plane-polarized light photomicrograph displaying the radiating habit of calcite fibers in the botryoid and the equant habit of the replacement spar. **B.** Cathodoluminescence photomicrograph demonstrates the contrast in luminescent character of the two calcite generations. The luminescence of the botryoidal calcite is much higher than that of the spar, and exhibits an outward decrease in brightness. **C.** Interpretive sketch of same view.

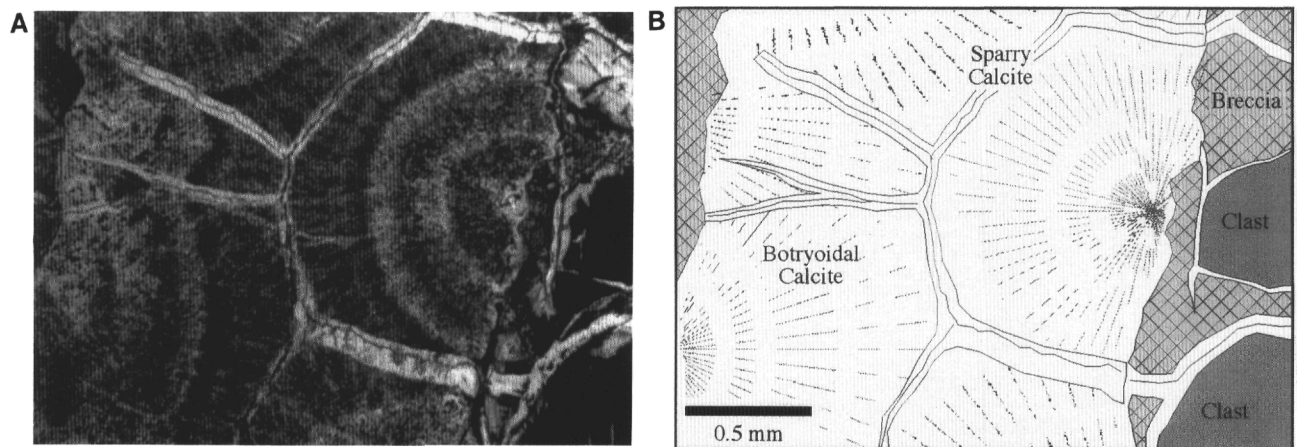


Figure 5. Botryoidal calcite completely filling a small vein in Sample 149-899B-16R-2, 102-105 cm. Variations in density of inclusions during growth of radial fibers result in concentric zones of inclusions. Subsequent fractures at the botryoid terminations are filled by clear, sparry calcite, which is continuous with fibrous veins in the wall. Clasts within the breccia are encircled by the fibrous veins. **A.** Plane-polarized light photomicrograph. **B.** Interpretive sketch.

to predate the calcite vein filling in the breccias at Site 897 (e.g., phyllosilicates, possible chlorite and smectite, and fibrous quartz; Figs. 8, 9), whereas others apparently postdate at least some of the calcite phases (e.g., brucite; Sample 149-897D-17R-4, 110-114 cm). Other phases, such as the ubiquitous oxides present among the calcite phases, clearly are deposited synchronously and are very useful for unraveling textural relationships and timing. Further discussion of the relationships between these phases and the calcite occurrences is deferred to discussion of chemical analyses (Milliken and Morgan, this volume).

Crack-seal Textures

This textural examination has revealed striking evidence for repeated fracture, vein opening, and resealing by subsequent precipita-

tion, yielding distinctive vein complexes and crosscutting relationships. In many tectonically active settings, such crack-seal textures preserve a clear record of incremental strain, which can be read in the context of a relatively consistent stress regime (e.g., Durney and Ramsay, 1973; Fisher and Brantley, 1992). A remarkable feature of the textures observed here is the apparent inconsistency, and consequent complexity, of these kinematic events. Certain fracture events appear to have followed a pattern, such as the repeated fracturing of existing vein complexes, which must define a plane of weakness (Fig. 10A-C). Others display fractures that crosscut each other in a poorly defined manner, suggesting alternating stress conditions (Fig. 10C-E). The complexity of these features is often not revealed under plane light, but may be clearly displayed by cathodoluminescence imaging (Fig. 10).

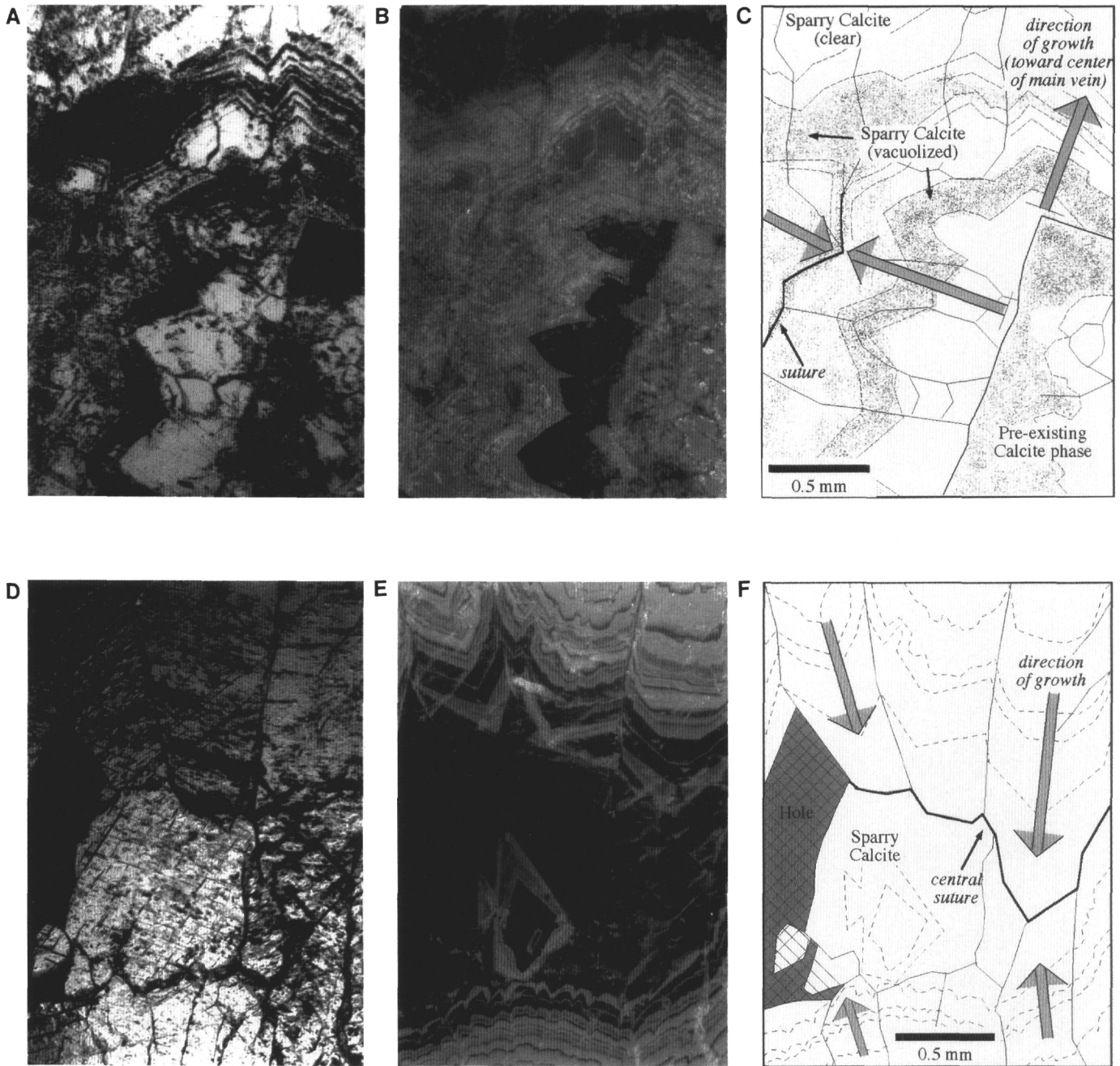


Figure 6. Sparry calcite vein filling, common to zoned veins at both Sites 897 and 899, from Sample 149-899B-18R-2, 135-139 cm. **A.** Plane-polarized light photomicrograph of inclusion-rich domain near the vein wall (not shown, but to lower right of photograph), showing complicated sawtooth growth patterns and inclusion banding at intersection with secondary zoned vein; calcite crystals initially grew outward from the vein walls and a preexisting calcite phase, simultaneously filling the secondary vein (at left) and main vein (at top). Once the secondary vein was sealed, crystal growth continued in the main vein. **B.** Cathodoluminescence photomicrograph of same view, showing high- to low-luminescent zones corresponding to bands of inclusions. **C.** Interpretive sketch of same view. Arrows show directions of mineral growth; dashed form lines show luminescent zoning patterns. **D.** Plane-polarized light photomicrograph of clear, coarse, bladed calcite near the center of the vein; grain boundaries stand out in relief, but are not otherwise distinguished (black hole to left is open porosity). **E.** Cathodoluminescence photomicrograph of same view, showing fine, rhythmic brightness zoning, grading to nonluminescent calcite near the center of vein. **F.** Interpretive sketch of same view, showing directions of growth, and position of central suture (symbols the same as in C).

DISCUSSION

This petrographic study of calcite veins at Sites 897 and 899 has revealed two distinctive features that direct our discussion of the tectonic and environmental conditions of their formation: first, vein opening and precipitation proceeded through multiple dilational steps, with little systematic organization in terms of fracture orienta-

tion or mineral growth; second, mineralization in open veins occurred through a progression of carbonate precipitation events, from prismatic aragonite, followed by botryoidal, fibrous calcite, and, finally, by bladed sparry calcite, with the last precipitation event involving the opening and filling of clastic veins.

The multiple deformational events led to the opening and maintenance of large fractures, which argue for overall dilation of the rock

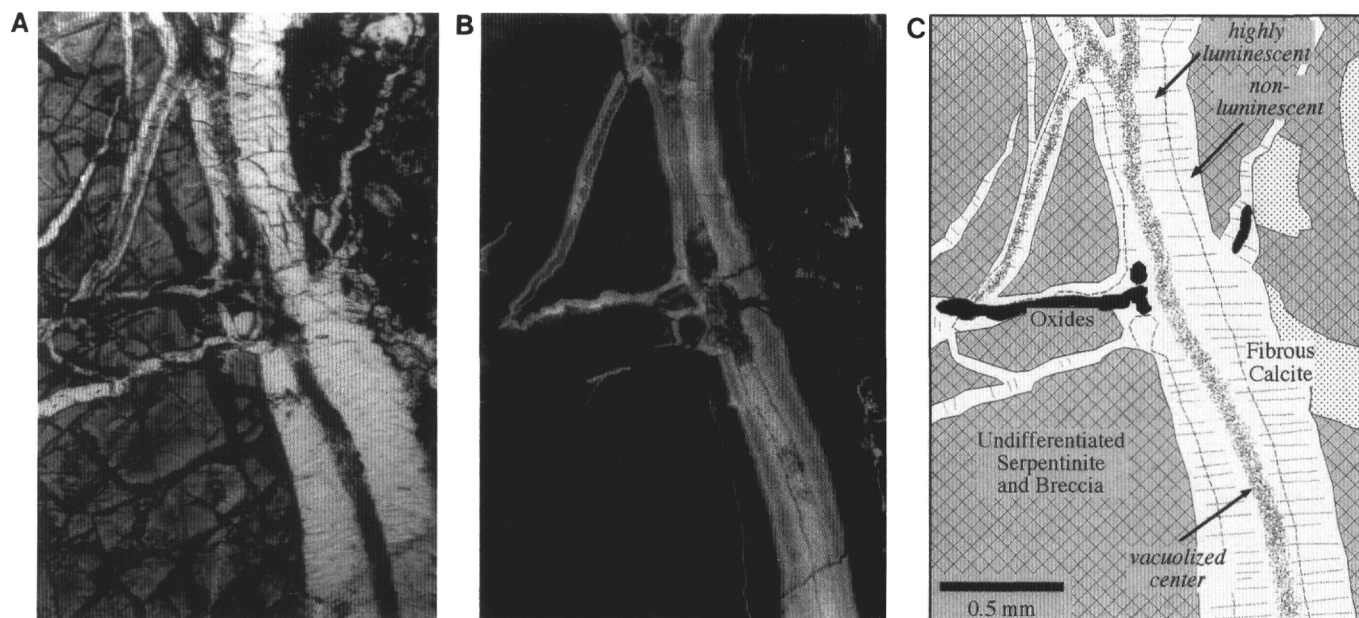


Figure 7. Fibrous veins in Sample 149-899B-16R-2, 69-72 cm, representing a common vein type at both Sites 897 and 899. **A.** Plane-polarized light photomicrograph showing fibrous calcite veins with distinct vacuolized calcite near their centers; fibers are oriented approximately perpendicular to the vein walls. **B.** Cathodoluminescence image of same view, showing nonuniform luminescence across the veins; the vacuolized cores are highly luminescent; the adjacent growth displays moderate and relatively uniform luminescence, but shows a sharp transition into nonluminescent calcite at the vein margins. Crosscutting of the luminescent calcite by nonluminescent calcite indicates antitaxial growth of the fibers. **C.** Interpretive sketch of same view. See Figure 6 caption for explanation of symbols.

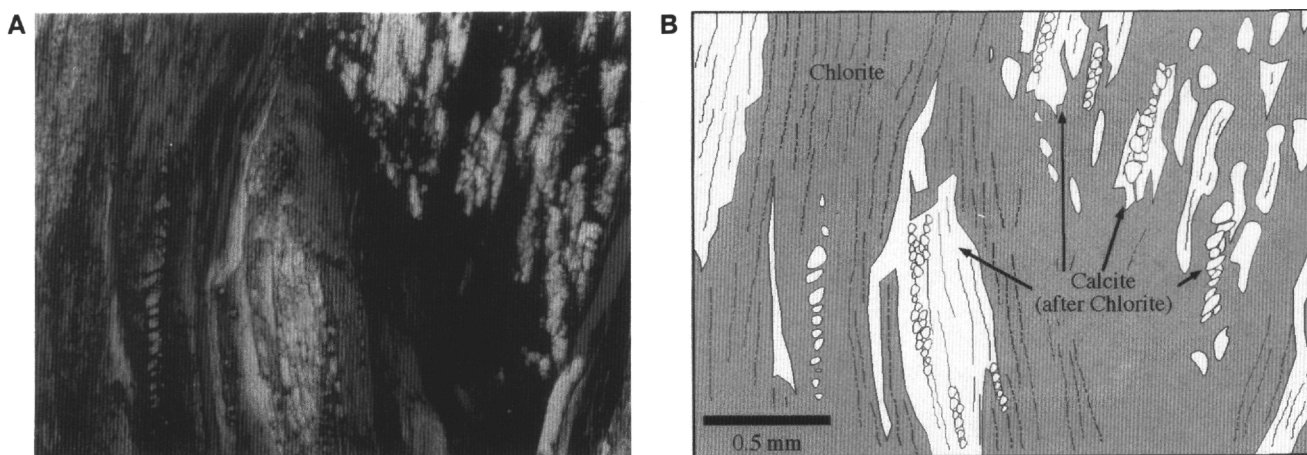


Figure 8. Massive, fibrous calcite intimately intergrown and apparently replacing primary chlorite in Sample 149-899B-18R-5, 58-62. **A.** Plane-polarized light photomicrograph demonstrating that the fibrous habit of the calcite appears to mimic that of the chlorite, to the extent that kinks in the chlorite are preserved. Calcite also occurs as small beads apparently nucleating within and at the margins of the chlorite fragments. **B.** Interpretive sketch of the same view.

mass. There is no evidence for subsequent collapse of these fractures (e.g., penetration, pressure solution fabrics; Fisher and Brantley, 1992), which might occur if the fractures were supported by high transient fluid pressures. The picture presented of discrete fracturing events, followed by long periods of carbonate precipitation, points to discontinuous, intermittent deformation. The overall picture supports a series of dilational events which took place in a setting of regional and/or local extension, consistent with near-surface brittle deformation. Perhaps these events correspond to deformation late in the rifting process, responsible for the uplift of the regional basement highs inferred to have postdated the deposition of the mass flow units found above basement at both sites (e.g., Shipboard Scientific Party, 1994a, b).

The culminating deformational event, at least in the samples examined here, corresponds to the brittle fracture and opening of the micrite-filled veins, possibly associated with the generation of the in situ breccias at Site 897. By analogy with neptunian veins observed in other extensional settings (Smart et al., 1987; Winterer et al., 1991), these features may be interpreted to reflect very late, near surface fracture of the exposed ultramafic basement (e.g., Lagabrielle and Auzende, 1982), possibly leading to gravitational instabilities: slumping, slope failure, and generation of landslides. It is not outside the realm of possibility that late dilational events, similar to those preserved by the micrite-filled veins at Site 897, were responsible for the ultimate fragmentation and collapse of the serpentinitized peridotite now preserved in the breccia units at Site 899 (Gibson, Milliken, and

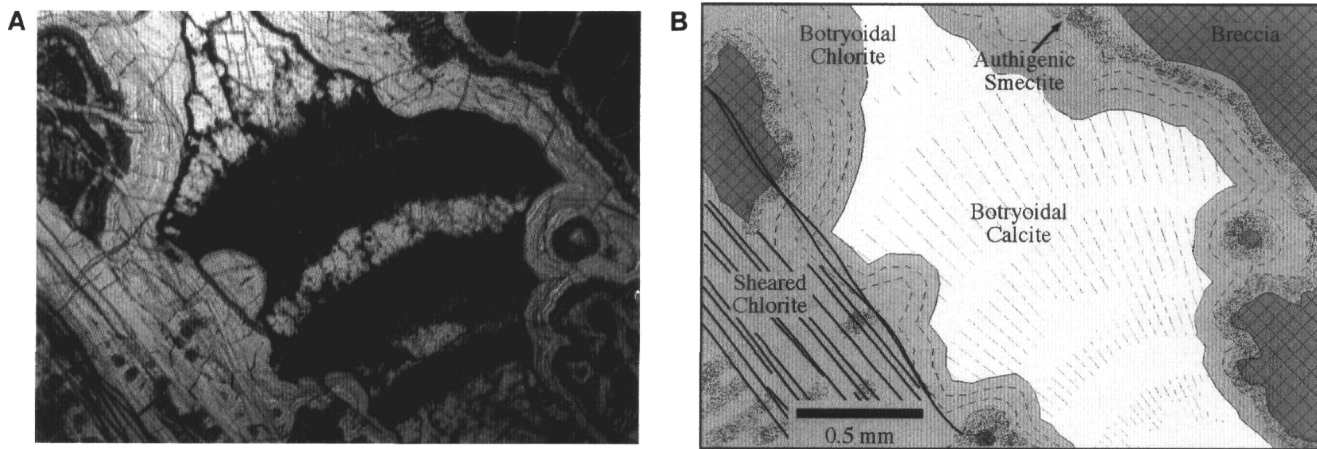


Figure 9. Botryoidal calcite filling a cavity in a chlorite-filled vein, Sample 149-899B-20R-2, 16-20 cm. **A.** Plane-polarized light photomicrograph. Chlorite displays an unusual botryoidal and isotropic habit near the margins of the vein, as evidenced by fine, concentric banding; crystal size is observed to coarsen toward the center of the vein (not shown). Chlorite also occurs in a planar habit at the lower left, crosscutting the botryoidal phase; parallel, high-relief bands that occur in this zone, as well as near the vein walls, may be composed of authigenic smectite. The infilling calcite apparently postdates the chlorite. **B.** Interpretive sketch of the same view.

Morgan, this volume), which may account for the relative dearth of micrite-filled veins at Site 899. In this scenario, the postdepositional veins sampled from the breccia units at Site 899 do not correlate directly with those at Site 897 (consider for example, the absence of the complex, aragonite-bearing veins at Site 899), despite the textural similarities at the two sites.

The mineralogical and morphologic progression identified here suggests that conditions of carbonate precipitation varied during filling of the veins. Conditions that favor the growth of one carbonate phase or habit at the expense of others have long been debated (e.g., Folk, 1974; Given and Wilkinson, 1985; Burton, 1993). Warm water temperatures, high Mg/Ca ratios, high salinity, and high carbonate concentrations have commonly been correlated with precipitation of aragonite; a hydrothermal origin is invoked to explain acicular aragonite observed in serpentinitic deposits from seamounts in the Mariana forearc setting (Lagabrielle et al. 1992). Chemical and thermal conditions associated with fibrous, botryoidal calcite occurrences are similar (Folk, 1974). Some would argue that botryoidal calcite actually represents a replacement texture of acicular radiating aragonite (e.g., Ross, 1991). More equant or bladed sparry calcite has been correlated with cooler, deeper marine or meteoric settings, typically with low Mg, and carbonate concentrations (Folk, 1974; Burton and Walter, 1987).

In an accompanying chemical study of the carbonate veins examined here, Milliken and Morgan (this volume) explored the correlations between carbonate morphology and the trace-elemental and isotopic signatures. Curiously, analyses designed to highlight just such chemical and thermal trends among the vein-filling phases instead demonstrate a relatively uniform fluid source, consistent with relatively low temperatures (10°-20°C), apparently representing an Early Cretaceous seawater only slightly modified by interaction with serpentinitized peridotite basement (Milliken and Morgan, this volume). It is possible that some of the earlier vein-filling carbonates have been largely replaced, in the process losing their distinctive chemical, thermal, or temporal signatures, and acquiring those of the ambient fluid at the time of replacement. Replacement, however, would tend to erase primary directional growth textures, yielding more uniform, equant calcite (e.g., Bathurst, 1975; Ross, 1991). This is evidently the case for the examples of relict aragonite, which have been replaced by clear, equant calcite with very uniform luminescence. Certain occurrences of botryoidal calcite also show a more equant calcite habit; the botryoidal form is only evident from concentric bands of inclu-

sions. Generally, however, the radiating fibrous patterns and fine inclusion and luminescent zoning in the botryoids point to the preservation of primary mineralogy. There is little evidence that the bladed, sparry calcites have undergone any replacement, as the fine details of the crystal habit and luminescent zoning are extremely well preserved (e.g., Fig. 6). These observations confirm that most of the carbonate chemistries that we have documented accurately record primary precipitation conditions.

Perhaps the conditions controlling carbonate morphology and phase depended more on precipitation rate (e.g., Given and Wilkinson, 1985). Given the intermittent history of deformation in these rocks, the width and stability of open fractures may have varied over time, directly controlling the flux of carbonate-bearing fluids through the system, and indirectly controlling the precipitation rate. Tectonically induced fractures, activating preexisting planes of weakness in the rock, may have introduced an extensive system of open veins, through which flow rates were quite high; aragonite may have been the favored phase, followed by botryoidal, fibrous calcite. Progressive narrowing of the veins, by the growth of vein-filling phases unaccompanied by successive widening events, may have favored the growth of coarse, bladed calcite. Collapse and in situ brecciation of the rock, possibly accompanied by high fluid flux, is inferred to have been one of the latest stages of deformation, at least at Site 897; the introduction of micrite into the fractures may indicate a sudden increase in precipitation rates (Folk, 1974) associated with the injection of fluids and remobilized calcite into the fractures. These features were subsequently cemented by sparry calcite.

CONCLUSION

Several conclusions can be drawn from this petrographic study of carbonate veins in serpentinitized basement cores from Sites 897 and 899.

1. Veins demonstrate an extensive history of fracture and refraction, consistent with local dilation of the basement rocks in a rift-related extensional setting. The progression in vein types suggests the early formation of large, open fractures, which were sealed by various carbonate phases and subsequently re-fractured during renewed deformational activity. Fracture orientations appear to be largely controlled by local stress

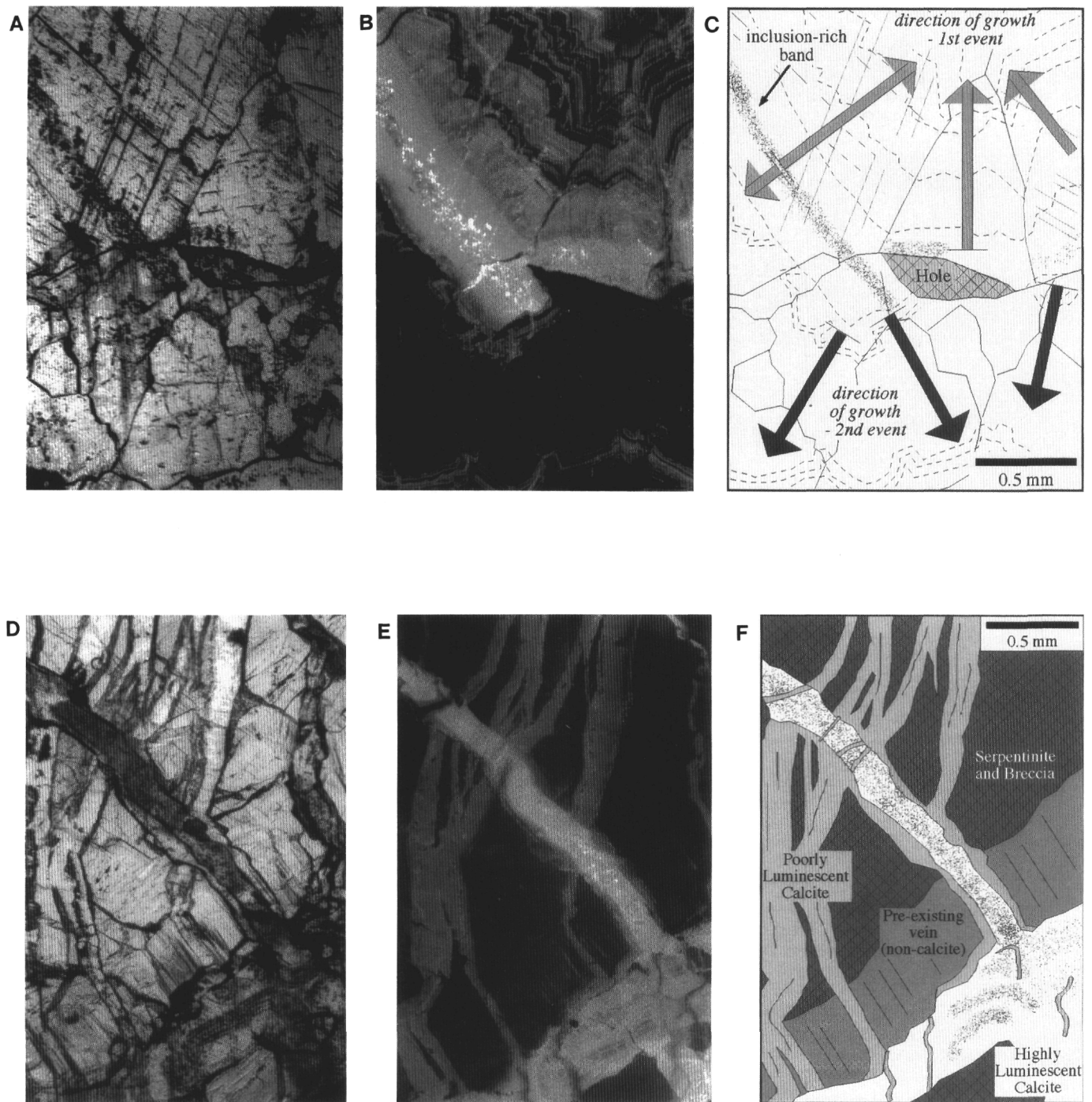


Figure 10. Crack-seal textures in calcite veins. **A.** Plane-polarized light photomicrograph of Sample 149-899B-18R-5, 58-62 cm, showing coarse, blocky crystals with different optical orientations (note cleavage planes). Grain boundaries stand out in relief, and a narrow, inclusion-rich band is observed to transect the boundaries. **B.** Cathodoluminescence photomicrograph of same view showing the distinct truncation of a highly luminescent band of calcite cored by the inclusion-rich band, and a contrast in luminescence on either side of the band. **C.** Interpretive sketch of same view. Two episodes of calcite precipitation are suggested. The first event, symmetric about the inclusion-rich band, produced highly luminescent, zoned calcite (gray arrows); a second, postfracture, event led to syntaxial growth of poorly luminescent, finely zoned calcite (black arrows). See Figure 6 caption for explanation of symbols. **D.** Plane-polarized light photomicrograph of Sample 149-899B-19R-2, 111-114 cm, showing complicated crosscutting relationships among different vein generations. The large vacuolized vein at the lower right corner appears continuous with a vein with a vacuolized core that transects the image, and appears to crosscut clear, vertical veins. **E.** Cathodoluminescence photomicrograph demonstrates greater complexity; the less luminescent, vertical veins appear to overprint the apparently later, more luminescent vacuolized veins. This apparent contradiction may arise from multiple, alternating vein-generating events. **F.** Interpretive sketch of same view.

- variations, perhaps associated with preexisting basement fabric, rather than regional tectonic stress conditions.
- The last apparent fracture and vein-filling event, most pronounced at Site 897, resulted in the development of crosscutting micrite-filled veins, similar in character to neptunian veins associated with dilation and fragmentation of rocks, and sedimentary influx in a near-seafloor environment. These features appear to correlate with in situ brecciation of the rocks, which may have introduced much of the internal sediment. The micrite-filled veins are interpreted to reflect late-stage gravitational collapse of the basement rock subsequent to uplift.
 - Petrographic observations reveal a temporal progression in carbonate phase and morphology, from precipitation of aragonite in large, open fractures, followed by fibrous, botryoidal calcite, and finally by coarse, bladed sparry calcite. There is little evidence to support replacement of most of these phases. Variations in carbonate morphology, without corresponding variations in calcite chemistry, suggest that precipitation conditions and rates in the fractures may have been controlled by fluid flow rates through the veins.

ACKNOWLEDGMENTS

This work was supported by grants USSSP022 to Morgan and USSSP012 to Milliken. We thank Larry Cathles for the use of his cathodoluminescence equipment and Maura Weathers and Bill Bassett for the use of their microscopic equipment and their space. An anonymous reviewer provided some helpful comments for the revision of the manuscript.

REFERENCES

- Agrinier, P., Mével, C., and Girardeau, J., 1988. Hydrothermal alteration of the peridotites cored at the ocean/continent boundary of the Iberian Margin: petrologic and stable isotope evidence. *In* Boillot, G., Winterer, E.L., et al., *Proc. ODP, Sci. Results*, 103: College Station, TX (Ocean Drilling Program), 225-234.
- Bathurst, R.G.C., 1975. *Carbonate Sediments and Their Diagenesis* (2nd ed.): Amsterdam (Elsevier).
- Boillot, G., Girardeau, J., and Kornprobst, J., 1988. Rifting of the Galicia Margin: crustal thinning and emplacement of mantle rocks on the seafloor. *In* Boillot, G., Winterer, E.L., et al., *Proc. ODP, Sci. Results*, 103: College Station, TX (Ocean Drilling Program), 741-756.
- Bonatti, E., Emiliani, C., Ferrara, G., Honnorez, J., and Rydell, H., 1974. Ultramafic-carbonate breccias from the equatorial Mid Atlantic Ridge. *Mar. Geol.*, 16:83-102.
- Bonatti, E., Lawrence, J.R., Hamlyn, P.R., and Breger, D., 1980. Aragonite from deep sea ultramafic rocks. *Geochim. Cosmochim. Acta*, 44:1207-1214.
- Burton, E.A., 1993. Controls on marine carbonate cement mineralogy: review and reassessment. *Chem. Geol.*, 105:163-179.
- Burton, E.A., and Walter, L.M., 1987. Relative precipitation rate of aragonite and Mg Calcite from seawater: temperature or carbonate ion control? *Geology*, 15:111-114.
- Durney, D.W., and Ramsay, J.G., 1973. Incremental strains measured by Syntectonic crystal growth. *In* De Jong, K.A., and Scholten, R. (Eds.), *Gravity and Tectonics*: New York (Wiley), 67-96.
- Fisher, D.M., and Brantley, S.L., 1992. Models of quartz overgrowth and vein formation: deformation and episodic fluid flow in an ancient subduction zone. *J. Geophys. Res.*, 97:20043-20061.
- Folk, R.L., 1974. The natural history of crystalline calcium carbonate: effects of magnesium content and salinity. *J. Sediment. Petrol.*, 44:40-53.
- Folk, R.L., and McBride, E.F., 1976. Possible pedogenic origin of Ligurian ophicalcite: a mesozoic calichified serpentinite. *Geology*, 4:327-332.
- Früh-Green, G.L., Weissert, H., and Bernoulli, D., 1990. A multiple fluid history recorded in Alpine ophiolites. *J. Geol. Soc. London*, 147:959-970.
- Gillis, K.M., and Robinson, P.T., 1988. Distribution of alteration zones in the upper oceanic crust. *Geology*, 16:262-266.
- Given, R.K., and Wilkinson, B.H., 1985. Kinetic control of morphology, composition and mineralogy of abiogenic sedimentary carbonates. *J. Sediment. Petrol.*, 55:109-119.
- Hsü, K.J., 1983. Neptunian dikes and their relation to the hydrothermal circulation of submarine hydrothermal systems. *Geology*, 11:455-457.
- Kimball, K.L., and Evans, C.A., 1988. Hydrothermal alteration of peridotite from the Galicia Margin, Iberian Peninsula. *In* Boillot, G., Winterer, E.L., et al., *Proc. ODP, Sci. Results*, 103: College Station, TX (Ocean Drilling Program), 241-251.
- Lagabrielle, Y., and Auzende, J.-M., 1982. Active in situ disaggregation of oceanic crust and mantle on Gorrige Band: analogy with ophiolitic massives. *Nature*, 297:490-493.
- Lagabrielle, Y., Karpoff, A.-M., and Cotten, J., 1992. Mineralogical and geochemical analysis of sedimentary serpentinites from Conical Seamount (Hole 778a): implication for the evolution of serpentine seamounts. *In* Fryer, P., Pearce, J.A., Stokking, L.B., et al., *Proc. ODP, Sci. Results*, 125: College Station, TX (Ocean Drilling Program), 325-342.
- Ross, D.J., 1991. Botryoidal high magnesium calcite cements from the upper Cretaceous of the Mediterranean region. *J. Sediment. Petrol.*, 61:349-353.
- Sawyer, D.S., Whitmarsh, R.B., Klaus, A., et al., 1994. *Proc. ODP, Init. Repts.*, 149: College Station, TX (Ocean Drilling Program).
- Shipboard Scientific Party, 1994a. Introduction. *In* Sawyer, D.S., Whitmarsh, R.B., Klaus, A., et al., *Proc. ODP, Init. Repts.*, 149: College Station, TX (Ocean Drilling Program), 5-10.
- , 1994b. Site 897. *In* Sawyer, D.S., Whitmarsh, R.B., Klaus, A., et al., *Proc. ODP, Init. Repts.*, 149: College Station, TX (Ocean Drilling Program), 41-113.
- , 1994c. Site 899. *In* Sawyer, D.S., Whitmarsh, R.B., Klaus, A., et al., *Proc. ODP, Init. Repts.*, 149: College Station, TX (Ocean Drilling Program), 147-209.
- Smart, P.L., Palmer, R.J., Whitaker, F., and Wright, V.P., 1987. Neptunian dikes and fissure fills: an overview and account of some modern examples. *In* James, N.P., and Choquette, P.W. (Eds.), *Paleokarst*: New York (Springer-Verlag), 149-163.
- Weissert, H., and Bernoulli, D., 1984. Oxygen isotopic composition of calcite in Alpine ophicalcites: a hydrothermal or Alpine metamorphic signal? *Eclogae Geol. Helv.*, 77:29-43.
- Whitmarsh, R.B., Miles, P.R., and Mauffret, A., 1990. The ocean-continent boundary off the western continental margin of Iberia, I. Crustal structure at 40°30'N. *Geophys. J. Int.*, 103:509-531.
- Whitmarsh, R.B., Pinheiro, L.M., Miles, P.R., Recq, M., and Sibuet, J.C., 1993. Thin crust at the western Iberia ocean-continent transition and ophiolites. *Tectonics*, 12:1230-1239.
- Winterer, E.L., Metzler, C.V., and Sarti, M., 1991. Neptunian dykes and associated breccias (Southern Alps, Italy and Switzerland): role of gravity sliding in open and closed systems. *Sedimentology*, 38:381-404.

Date of initial receipt: 5 December 1994

Date of acceptance: 19 July 1995

Ms 149SR-230